Research on Engineering Structures & Materials
www.jresm.org
Research Group

Research Article

Shear strength, CBR, and interface interaction of pumice-modified clay reinforced with Geostrip: A large-scale laboratory study

Sami S. Jasim [*,1,a], Madhat Shakir Al-Soud [2,b], Qais S. Banyhussan [3,c]

[1]*Dept. of Civil Eng.g, Mustansiriyah University, Baghdad 10052, Iraq*
[2]*Dept. of Civil Eng.g, College of Engineering, Al-Mustansiriya University, Baghdad 10052, Iraq*
[3]*Dept. of Highway and Transportation Eng., College of Engineering, Al-Mustansiriya University, Baghdad 10052, Iraq*

Article Info

Article History:

Received 01 July 2026

Accepted 22 July 2026

Keywords:

Pumice;
Soil stabilization;
Large-scale direct shear test;
Geostrip reinforcement;
California bearing ratio;
Interface interaction coefficient;
Sustainable geotechnics;
Clay modification

Abstract

Clayey soils are challenging in geotechnical engineering because of their high compressibility, moisture sensitivity, and low shear strength. This study investigates lightweight and sustainable pumice, locally termed Ponza, for stabilizing clayey soil collected from Al-Amiriya, Baghdad, Iraq. Pumice was incorporated at replacement ratios of 10%, 20%, 30%, 40%, and 50% by dry mass. For each mixture, the dry constituents were blended, mixed with water at the corresponding optimum moisture content, and compacted before testing; CBR specimens were then soaked for 72 h. The experimental program included modified Proctor compaction, soaked California Bearing Ratio tests, and large-scale direct shear tests under normal stresses of 25, 50, and 75 kPa for unreinforced and Geostrip-reinforced specimens. A 200-mm-wide shear box was selected to accommodate the 4.75–9.5 mm pumice particles and minimize particle-size and boundary effects. Increasing pumice content reduced the maximum dry density and produced an overall increase in optimum moisture content because of the lightweight and porous nature of pumice. CBR generally improved at higher pumice contents owing to greater particle interlocking and the development of a frictional load-bearing skeleton. The shear response gradually changed from cohesion to friction-controlled behavior. For unreinforced samples, the friction angle increased from 16.3° for natural clay to 31.0° for 50% pumice, and cohesion decreased from 19.69 kPa to 10.50 kPa. Average interface interaction coefficients of 0.94–0.99 are shown to be efficient at stress transfer and compatible with the clay-pumice mixtures and Geostrip reinforcement.

1. Introduction

Clayey soils are challenging geotechnically in roads, embankments, retaining structures, and shallow foundations because moisture-induced changes in soil fabric can cause settlement, deformation, and loss of bearing capacity and shear strength [1–6]. These problems have led to stabilization and reinforcement in weak fine-grained soils together. Pumice is a porous volcanic lightweight aggregate characterized by low specific gravity, high water absorption, and a rough, angular surface. These properties can lead to a lower weight of compacted fills while modifying particle arrangement, frictional resistance, and interparticle interlocking [7,8,26,29]. Compared to cement or lime-based treatment, coarse pumice is more of a physical change to the soil skeleton than chemical stabilization. However, its environmental and economic benefits are highly dependent on local availability, processing, and transport. Recently, pumice in fine-grained soils

*Corresponding author: sam.albarahan@uomustansiriyah.edu.iq
[a]orcid.org/0009-0005-1746-6311; [b]orcid.org/0000-0002-1293-3452; [c]orcid.org/0000-0002-5927-0633
DOI: http://dx.doi.org/10.17515/resm2026-1811me0701rs

has been investigated using different forms, particle sizes, and replacement ratios. Aljboori et al. [26] evaluated clay mixed with pumice-based lightweight aggregate at 10%, 30%, 40%, 50%, and 60% dry mass using conventional compaction, consolidation, and strength tests. Their findings showed that the increase in the lightweight aggregate content reduced soil density and increased the frictional contribution to strength gradually, but too much replacement disturbed the clay matrix. Saltan et al. [29] demonstrated the potential of pumice waste to improve poor clayey pavement subgrades with this approach. Nasiri et al. [30] explored 5–15% fine pumice powder in contaminated clay and found 10% to be a good content for long-term strength and microstructure improvement. However, the fine pumice powder under curing behavior is very different from the coarse pumice particles acting as a lightweight granular modifier. Most of the available literature on compaction, CBR, unconfined compressive strength, consolidation, or drained shear parameters is limited in terms of the direct evidence for pore-water-pressure response and improved interface behavior in coarse clay–pumice mixtures [26,29,30]. The Mohr–Coulomb approach of cohesion and internal friction angle of the shear strength is widely used in the analysis and design of foundations, slopes, embankments, and earth-retaining structures [11–14]. The cohesion may be decreased because the clay-to-clay bond is broken (see section 2.2 below) and the mobilized friction angle is increased because of the angularity of the pumice particles, surface roughness, dilation, and confinement-dependent interlocking of the clay matrix [24–26]. At low pumice contents, isolated coarse particles can form local voids and weaken the clay matrix in the presence of low compactive effort. This transition must therefore be assessed both in penetration resistance and shear-strength tests rather than through compaction alone.

In reinforced-soil systems, overall performance also depends on shear transfer along the soil–geosynthetic interface. Previous pullout and interface studies have shown that reinforcement geometry, soil type, and the contact condition between clay and geosynthetic reinforcement strongly influence the mobilized interaction resistance [9,10]. ParaWeb 2D is a polymeric strip reinforcement composed of high-tenacity polyester yarn tendons encased in a protective polyethylene sheath [27]. Compared with continuous sheet-type geosynthetics, discrete strips can be arranged at selected elevations and lengths to mobilize tensile resistance while adding little self-weight; however, their effectiveness depends directly on the resistance developed along the soil–strip interface [15–18,27]. Interface behavior is governed by adhesion, surface texture, moisture condition, particle size and arrangement, normal stress, reinforcement geometry, and the mechanical characteristics of the polymeric strip [15–20,31,32]. Chai and Saito [31] showed that the interface shear response of clayey soils varies with geosynthetic type and contact condition. Choudhary and Krishna [20] demonstrated that particle size and geosynthetic structure influence interface friction and interaction coefficients, while Muluti et al. [32] confirmed that the configuration of the critical interface affects both peak and large-displacement strength. Consequently, the interaction of ParaWeb 2D with clay–pumice mixtures cannot be inferred reliably from soil-only strength and must be evaluated directly at the soil–strip contact surface.

Because the soil–strip response must be measured directly, large-scale direct shear testing is particularly important for the 4.75–9.5 mm pumice fraction used in the present study. A small shear box may exaggerate particle-size and boundary effects, and individual coarse particles can disproportionately influence rotation, dilation, crushing, and measured shear resistance when the specimen dimensions are insufficient relative to the maximum particle size. Deiminiat et al. [28] demonstrated that the specimen-width-to-maximum-particle-size ratio significantly influences direct shear results for coarse materials. The 200-mm-wide box adopted in this study provides a width-to-maximum-particle-size ratio of approximately 21, thereby reducing the scale and boundary effects expected in a conventional small shear box.

The previous investigation [26] characterized clay–lightweight aggregate mixtures using smaller pumice particles and conventional-scale laboratory testing, without evaluating the ParaWeb soil–reinforcement interface under the present large-scale configuration. The current study builds upon this previous work by using a coarser pumice fraction of 4.75-9.5 mm, soaked California Bearing Ratio tests at three compactive efforts, and investigating the soil-soil and soil-ParaWeb interface shear behavior in a 200-mm-wide direct shear box at 25, 50, and 75 kPa. Hence, this paper is not only a retelling of the previous work, but is focused on the effect of the particle medium on the interface and the engineering ability of the lightweight clay-pumice mix. Therefore, the novelty of the present study is that it allows for the investigation of pumice modification, CBR performance, Geostrip reinforcement, and large-scale soil-geosynthetic interface in a single experimental setting. This paper fills the gap in the literature on the shear transfer between coarse pumice-modified clay and polymeric reinforcement strips by measuring the change of cohesion, friction angle, interface adhesion, and interaction coefficient with increasing pumice content.

This study aims to investigate the synergistic effects of pumice inclusion and ParaWeb 2D Geostrip reinforcement on compaction, bearing resistance, internal shear strength, and soil–strip interface behavior through large-scale testing, with particular emphasis on failure mechanisms and lightweight embankment and mechanically stabilized earth backfill applications. Because pore-water pressure was not directly measured in the present program, the reported interface interpretation is limited to the measured compaction, CBR, and direct-shear responses.

2. Materials and Methods

2.1. Temperature Gradient

The natural clay was collected from the Al-Amiriya area, western Baghdad, Iraq (33.299593° N, 44.272867° E), at a depth of 1.5–2.0 m. The soil was air-dried and pulverized before testing. Its physical and chemical properties are summarized in Table 1. The soil was classified as low-plasticity clay (CL), with a liquid limit of 30.5%, a plastic limit of 19.8%, and a plasticity index of 10.7%. The gradation comprised 85% fines passing the No. 200 sieve and 15% sand-sized material; the complete distribution is shown in Fig. 1. The specific gravity was 2.76, while the optimum moisture content and maximum dry density were 16% and 1.835 g/cm^3, respectively.

Table 1. Physical and chemical properties of the natural soil

Property	Value
Soil classification	CL
Specific gravity	2.76
Liquid limit (%)	30.5
Plastic Limit (%)	19.8
Plasticity index (%)	10.7
Maximum dry density (g/cm^3)	1.835
Optimum moisture content (%)	16
Sand%	15
Silt%	19
Clay%	66
pH	7.4
Sulfate content, SO_3 (%)	0.103
Gypsum content (%)	0.221
Chloride content, Cl^- (%)	0.031

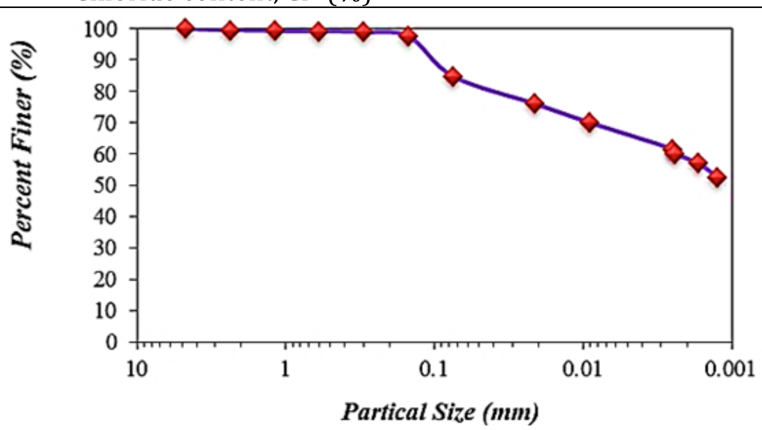

Fig. 1. Particle-size distribution curve of the natural clay

2.2 Pumice and Geostrip (ParaWeb 2D)

Pumice (locally termed Ponza) was imported from northern Iran and used as a lightweight granular additive. Pumice was incorporated at 10%, 20%, 30%, 40%, and 50% by dry mass of soil. The moist mixture was then homogenized before compaction and specimen preparation as shown in Fig. 2. Table 2 presents the measured physical and chemical properties of the material used in the experimental program. The aggregate was silica-rich, porous, and absorptive, characteristics that explain the reduction in mixture density and the non-monotonic water demand. ParaWeb 2D, as shown in Fig. 3, reinforcement consisted of high-tenacity polyester yarn tendons encased in a polyethylene sheath. The manufacturer reports an approximate strip width of 90 mm, thickness of 3 mm, and nominal ultimate tensile capacity of 75.4 kN per strip.

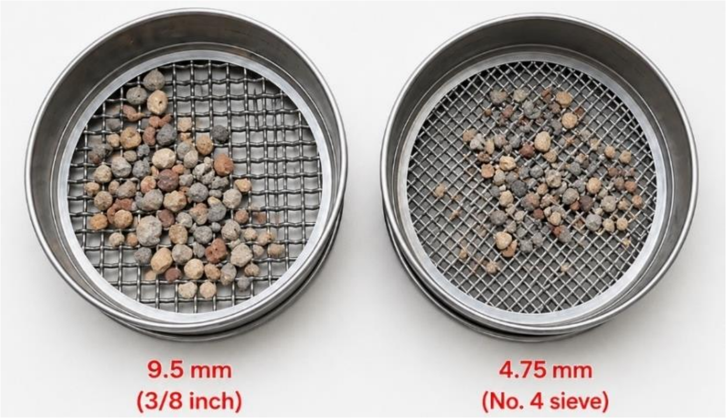

Fig. 2. Selected pumice fraction used in the study (passing 9.5 mm and retained on 4.75 mm sieve)

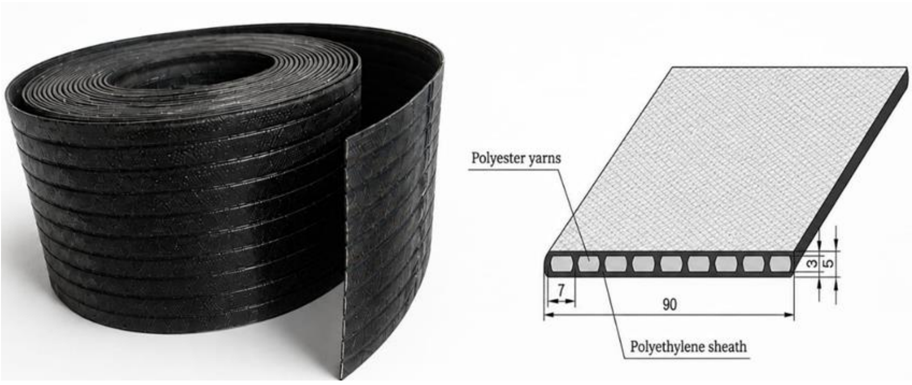

Fig. 3. ParaWeb 2D reinforcement strip and cross-sectional schematic (nominal strip width = 90 mm)

Table 2. Summary properties of the pumice used in this study.

Property	Value	Source/status
Selected particle-size range	4.75–9.5 mm	Present program
Specific gravity	1.931	Measured material property
Water absorption (%)	14.830	
Dry bulk density (kg/m^3)	995	
SiO_2 (%)	61.126	Chemical analysis
Al_2O_3 (%)	14.069	
Fe_2O_3 (%)	8.342	
CaO (%)	8.422	
MgO (%)	3.300	

2.3 Experimental Work

Physical model and index testing were performed at the Burj Babel Company for Studies and Scientific Research laboratories, whereas the large-scale direct shear testing was conducted at the Roads Laboratory, Mustansiriyah University.

2.3.1 Test Sample Preparation

Pumice was used as a coarse, lightweight granular modifier at replacement ratios of 10%, 20%, 30%, 40%, and 50% by dry mass of the natural soil. The pumice fragments were crushed and sieved, and the fraction that passed the 9.5 mm sieve and was retained on the 4.75 mm sieve was chosen. This very coarse fraction was chosen so as to preserve the lightweight aggregate character of pumice and to make it possible for the particles to have roughness, angularity, and mechanical interlocking in the clay matrix rather than to be treated as fine powder or chemical binder. The required dry masses of clay and pumice were mixed manually until the coarse particles were evenly distributed. The water that was the optimum moisture content of each mixture was then added gradually, and a visually homogeneous mixture without wet or dry zones to be found in the mixture was made. The specimens were prepared immediately after mixing, and there was no time for the water to be balanced. The same mixing and placement procedure was maintained for all specimens to minimize segregation and preparation variability.

2.3.2 Compaction Test

Modified Proctor compaction tests according to ASTM D1557-12(2021) (method C) were carried out to determine the maximum dry density (MDD) and optimum moisture content (OMC) of the natural clay and clay-pumice mixture. A 152.4 mm diameter mold with an approximate height of 116.4 mm was used for compacting the sample in five thick, roughly equal layers (in which each layer received 56 uniformly distributed blows from a 4.54-kg rammer falling through a height of 457 mm). The material was processed through the 19.0 mm (3/4-in.) sieve. While the standard Proctor test is often used for fine-grained soils with moderate compaction, the modified compactive effort is selected to take into account relatively high field compaction required for pavement subgrades, highway embankments, and reinforced backfill. The 152.4 mm mold was also chosen for the gravel-sized pumice to reduce particle size and boundary effects and to provide a good representative compaction response for clay-pumice mixtures. The modified compactive effort was applied to be about 2700 kNm/m^3.

2.3.3 California Bearing Ratio (CBR)

Soaked California Bearing Ratio (CBR) tests were generally done in line with ASTM D1883-21 except for the modified soaking period of 72 h and penetration rate of 1 mm/min. Clay-pumice mixtures of 0%, 10%, 20%, 30%, 40%, and 50% pumice were mixed with water at the appropriate optimum moisture content (OMC). Three samples for each mixture were prepared and compacted in five approximately equal layers using 10, 25, and 56 blows per layer in order to represent three compactive efforts. A 4.54 kg rammer (with two 2.27 kg surcharge weights) was used to compress each sample and was applied during penetration testing. The specimens were soaked in water for 72 h, during which vertical expansion was monitored using a dial gauge. The percentage swell was measured at the end of the soaking time. After soaking, the specimens were allowed to drain for about 15 min while maintaining the surcharge. Penetration testing was done at a fixed rate of 1 mm/min, and the loads were measured at the specified penetration depths. The CBR value was measured from the loads at 2.5- and 5.0-mm penetration in comparison to the standard loads.

2.3.4 Large-Scale Direct Shear

A large-scale direct shear apparatus was used in this work (Fig. 4) to apply normal stresses of 25, 50, and 75 kPa. The apparatus was manufactured by Banyhussan and is described in [21]. It consists of a lower rectangular shear box (200 × 250 × 100 mm) and an upper square shear box (200 × 200 × 100 mm). The larger lower box was used to maintain approximately the same overlap and shearing area during horizontal displacement, and reduce the area correction uncertainty of the conventional equal-sized shear box halves. There are two restraining arms to keep the upper box horizontal and the lower one vertical. The steel loading plate was pressed very hard to provide a normal stress level, and an electric jack was driven on the lower box to lift it up. The shear force was measured using the load cell with a 5-ton weight. The surface of the metal-to-metal contact and guiding surfaces were lubricated to minimize the friction and not to cause damage to the soil-soil or soil-Geostrip shear interface. For the reinforced specimens, one 90 mm wide ParaWeb 2D strip with a nominal tensile capacity of 75.4 kN was placed flat and centered to the horizontal shear plane. The longitudinal direction of the strip was aligned with the direction of shearing, and the strip was taut and free of folds in order to conform to the clay-pumice mixture. The soil mixtures were prepared at the optimum moisture contents. The dry mass of each mixture was calculated from the known internal volume of the shear box and the maximum dry density obtained from the Modified Proctor test according to Eq. 1.

$$Md = \rho_{d,target} Vb \tag{1}$$

Where Md is the required dry mass, ρ_(d,target)is the target dry density, and Vb is the specimen volume. The corresponding moist mass was determined from Eq.2:

$$Mmoist = Md(1 + w) \tag{2}$$

Where w is the optimum moisture content expressed as a decimal. The prepared moist mixture was divided into three approximately equal portions and placed in the shear box in three layers. Each layer was compacted by uniform manual tamping until the calculated total mass occupied the predetermined box volume, thereby achieving the target dry density. The same target density, layer thickness, and tamping procedure were maintained for all reinforced and unreinforced specimens to minimize variations in specimen density and pumice-particle distribution. After specimen preparation, the required normal stress was applied, and the displacement rate of 1 mm/min was adopted based on the operating procedure of the large-scale apparatus and the comparable testing program [21]. Shearing was continued to a horizontal displacement of 30 mm for each normal-stress level. Because the rate was not derived from specimen-specific consolidation measurements, the results are interpreted as rate-dependent shear parameters rather than strictly drained parameters.

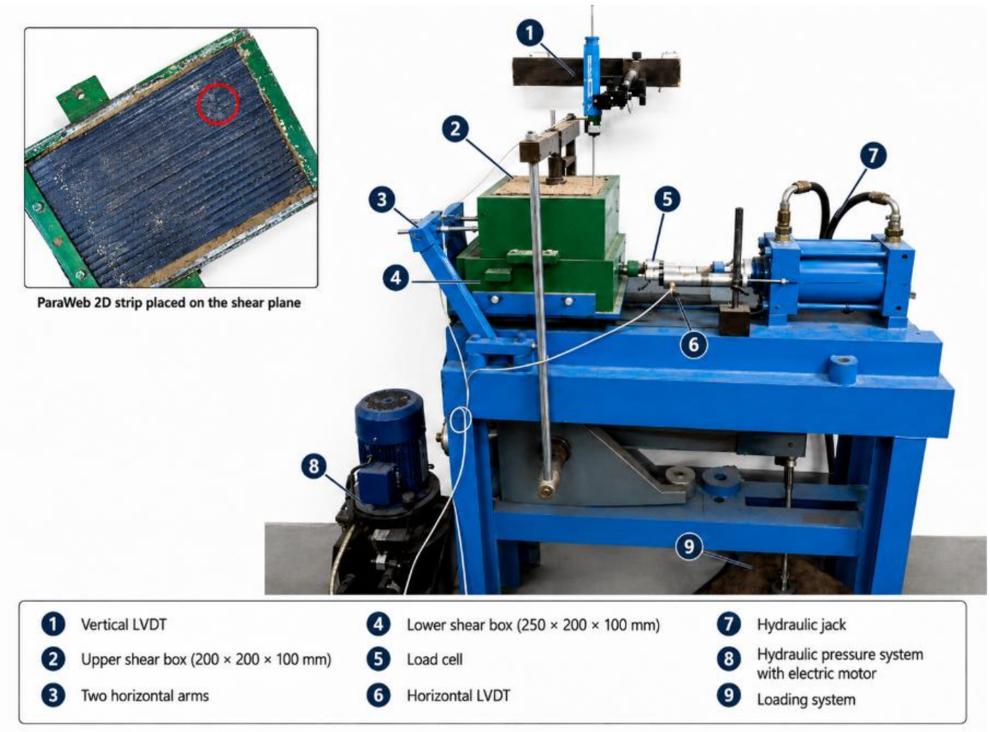

Fig. 4. Large-scale direct shear apparatus and numbered components

3. Results and Discussion

3.1. Compaction Results

The Modified Proctor results presented in Fig. 5 show that the natural clay achieved a maximum dry density (MDD) of approximately 1.84 g/cm^3 at an optimum moisture content (OMC) of 16%. Increasing the pumice content to 50% reduced the MDD to approximately 1.64 g/cm^3, corresponding to a reduction of about 10.9% relative to the natural clay. At the same replacement level, the OMC increased to approximately 17%, representing an increase of about 6.3%. But the OMC response was non-monotonic: the highest value of approximately 18.5% was reached at 40% pumice, which corresponds to an increase of about 15.6% from the natural soil and a slight decrease at 50% pumice. The decrease in MDD is mostly because of the low specific gravity and porous structure of pumice, whereas the change of OMC is caused by the competing effects of replacing water-requiring clay fines and water absorption by the porous pumice particles. For MSE applications, horizontal earth pressure is influenced simultaneously by the soil-mixture unit weight and the friction-dependent active earth-pressure coefficient as expressed in Eq. 3.

$$\sigma_h = Ka\, \gamma\, z \tag{3}$$

Where σ_h is active horizontal earth pressure, Ka is Rankine's active earth-pressure coefficient, $\gamma = \rho \times g$ is dry unit weight, ρd is dry density of the soil mixture, g is gravitational acceleration, z is the depth below the ground surface and z is the depth below the ground surface. For level backfill and zero wall friction, Rankine theory gives $Ka = \tan^2(45° - \varphi/2)$. So increasing the friction angle from 16.3° for natural clay to 31.0° for 50% pumice mixture reduces the active horizontal pressure from 0.562 to 0.320, a decrease of about 43%. At the same time, the dry density is decreasing from approximately 18.05 kN/m^3 to 16.09 kN/m^3 and the active horizontal pressure is decreasing from about 10.14 kPa for natural clay to 5.15 kPa for 50% pumice mixture; the total reduction is around 49%. So, the decrease in lateral pressure is a product of the lower unit weight and the nonlinear reduction of Ka with the higher friction angle, and not due to a constant Ka.

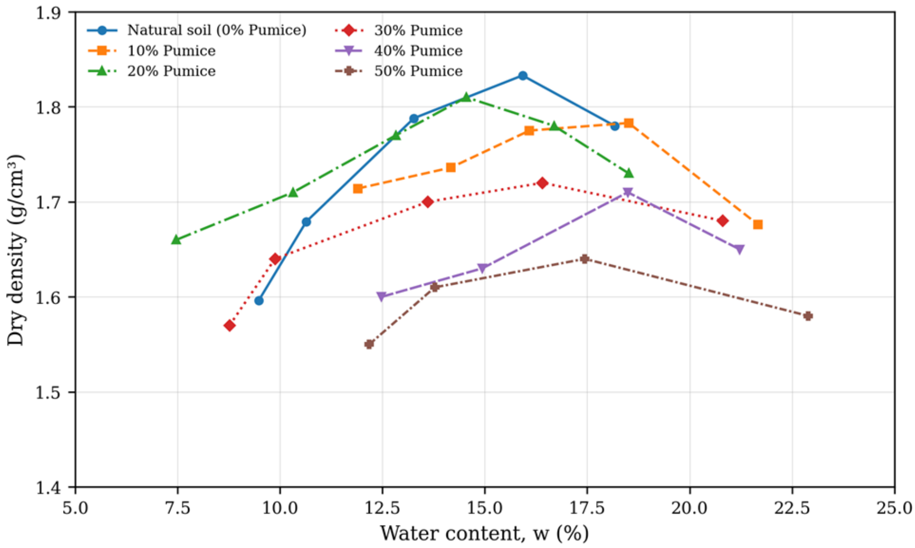

Fig. 5. Compaction curves for clay mixed with different pumice contents

3.2 CBR Test

Fig. 6 and Table 3 show the relationship between dry density and CBR for clay-pumice mixtures at three compactive efforts. For each mixture, the higher the compactive effort, the higher the dry density and the CBR, which proves that the compaction state is positively related to penetration resistance. The higher density makes for closer particle contact, less deformability and compressibility of specimens, and it also ensures that the internal load transfer path does not change as much as the pumice content. However, the response to the increase in pumice content is not monotonic, because the contribution of a cohesive clay matrix, contact between pumice and particles, void, and so on changes as the replacement ratio increases and the compactive effort increases. At 10 blows per layer of 10% pumice, a decrease in CBR from 1.400% for the natural soil to 0.531%. At that low energy, the small amount of coarse porous pumice might have interrupted the clay matrix without a continuous granular skeleton, and the local voids and incomplete seating of the pumice made them less resistant to penetration. With more compactive effort, the particles were embedded better, and CBR improved to 4.780% and 6.073% at 25 and 56 blows, respectively.

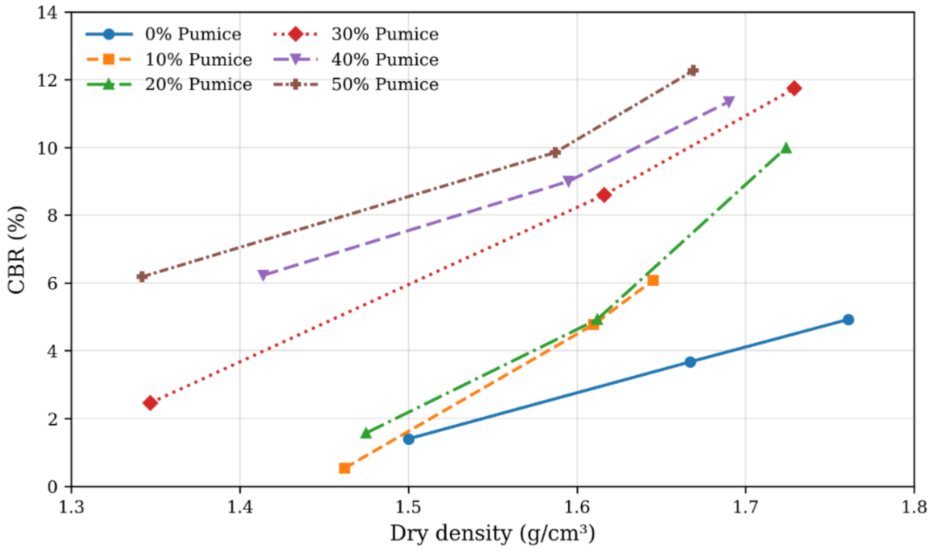

Fig. 6. Relationship between soaked CBR and dry density for the clay–pumice mixtures at three compactive efforts

Table 3. Soaked CBR results for the clay–pumice mixtures

Pumice content (%)	Number of blows per layer	Dry density (g/cm^3)	CBR (%)
0%	10	1.500	1.400
	25	1.667	3.670
	56	1.761	4.925
10%	10	1.462	0.531
	25	1.610	4.780
	56	1.645	6.073
20%	10	1.475	1.573
	25	1.612	4.924
	56	1.724	9.989
30%	10	1.347	2.463
	25	1.616	8.595
	56	1.729	11.739
40%	10	1.414	6.229
	25	1.595	9.000
	56	1.690	11.347
50%	10	1.342	6.181
	25	1.587	9.850
	56	1.669	12.265

The difference between the 30% and 40% pumice mixture was related to compactive effort. At 10 blows (6.229% versus 2.463%) and 25 blows (9.000% vs 8.595%) the mixture of 40% pumice had a higher CBR, whereas at 56 blows (11.739% vs 11.347%), it had a difference. At low and intermediate compactive efforts, the higher portion of coarse particles in the 40% mixture increased granular contact and penetration resistance. At the highest compactive effort, the 30%

mix seemed to have a more favorable balance of clay-matrix continuity and pumice interlocking. At this high content of pumice, enough clay fines were available to coat and seat the coarse pumice particles, fill particle voids, and rearrange them during compaction. At a higher content of pumice (40%), the amount of clay available per unit surface of coarse particles decreased, the clay fraction filled and lubricated less and less, and the particle seating and filling had less uniformity and localized voids, and at 56 blows, the CBR was slightly lower. As the difference between the 30% and 40% mixtures at 56 blows was small (3.3%) it should be considered only as a mixture structure effect and not a universal optimum content. The 50% mixture produced the highest CBR at 25 and 56 blows (9.850% and 12.265%) while the 40% mixture was slightly higher at 10 blows, which confirms that the preferred pumice content depends on the compactive effort. At higher pumice content, the overall improvement in CBR is attributed to the development of a stiffer load-bearing skeleton through more granular contact and mechanical interlocking. However, the porous and possibly crushable nature of pumice is likely to increase the compressibility of pumice and therefore the mixture gradation in a higher field stress. These limitations, together with the sensitivity of the clay-coating and void-filling mechanisms to mixing quality, should be considered when extrapolating these results to full-scale pavement and reinforced-backfill applications.

3.3. Large-Scale Direct Shear Tests

3.3.1 Group 1 (Unreinforced)

Fig. 7 presents the shear stress–horizontal displacement responses of the unreinforced clay–pumice mixtures under normal stresses of 25, 50, and 75 kPa. The natural clay exhibited a pronounced peak shear stress followed by post-peak softening, consistent with rupture of the cohesive clay fabric and subsequent particle rearrangement [21]. At normal stress 〖(σ〗_n)= 25 kPa, the natural clay produced the highest measured peak shear strength (26.4 kPa), whereas the 50% pumice mixture produced the highest values at σ_n = 50 and 75 kPa (40.0 and 55.75 kPa, respectively). The mixtures containing 10-30% pumice therefore represent a transition zone in which clay bonding, frictional sliding, and particle interlocking must be considered simultaneously, not a range of maximum shear strength. As the pumice content rose to 40-50% the response became more friction-controlled.

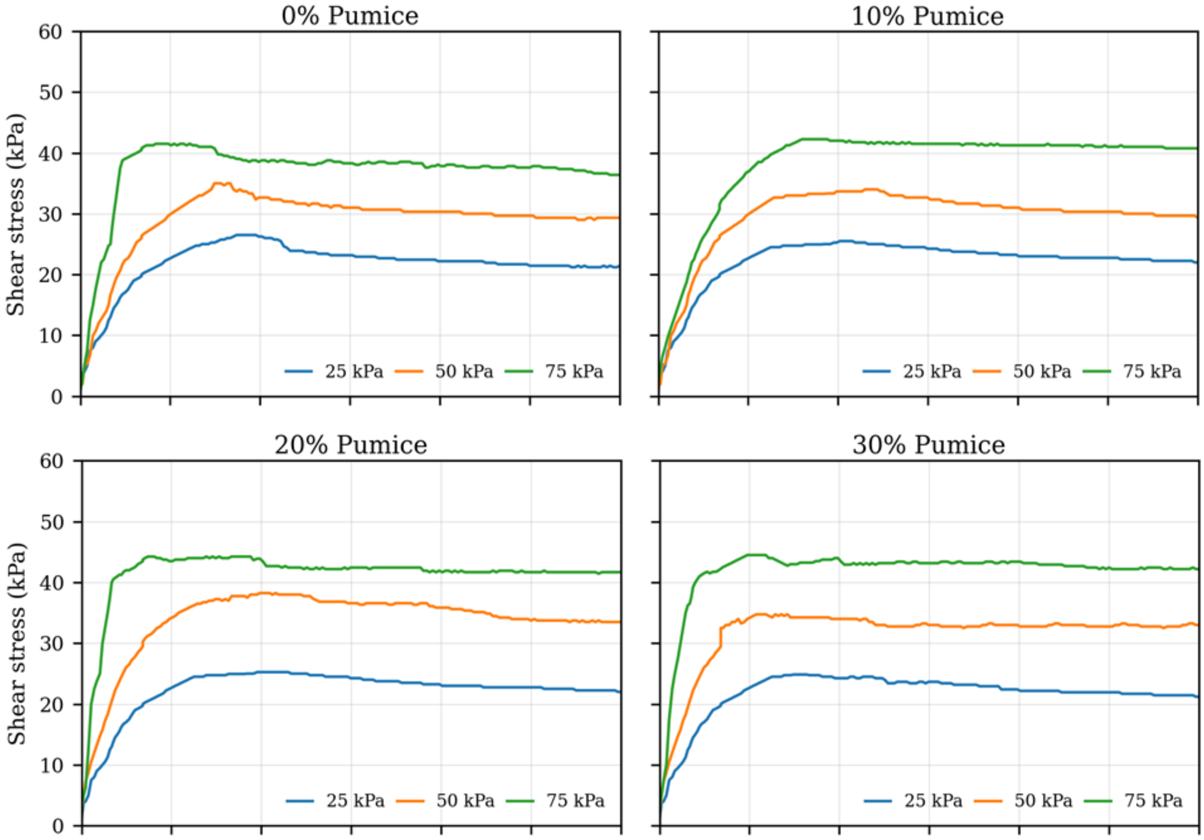

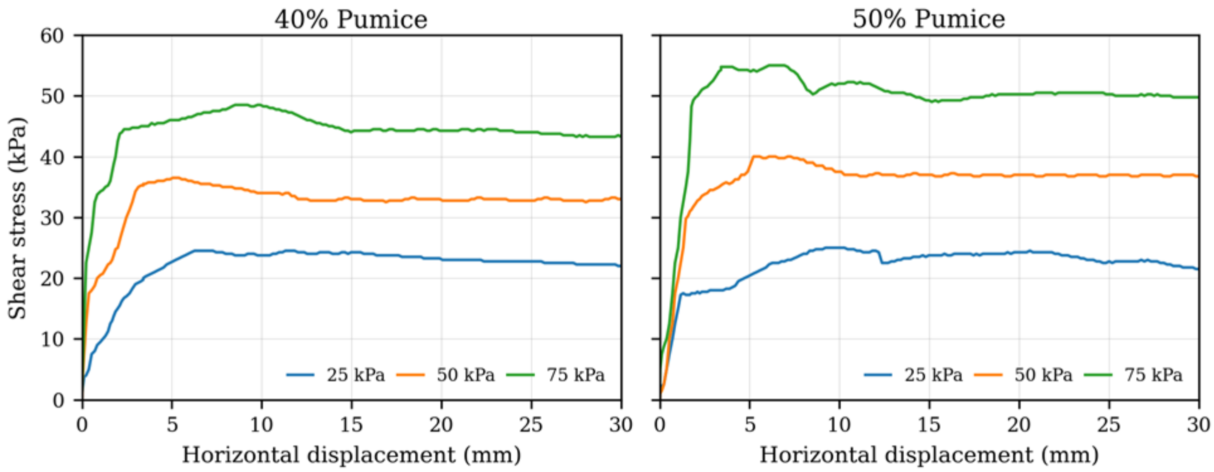

Fig. 7. Shear stress–horizontal displacement curves for unreinforced clay–pumice mixtures

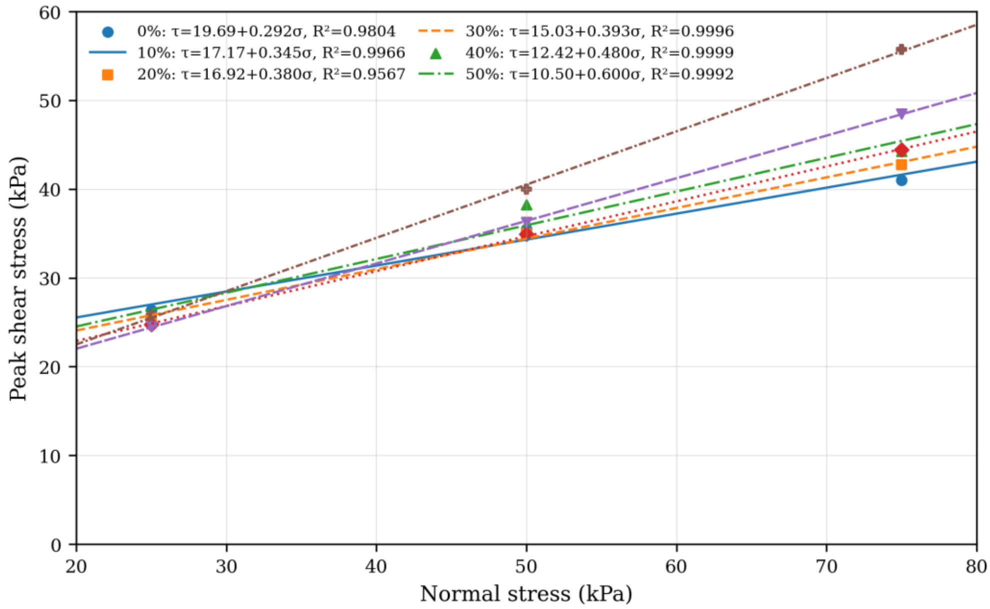

Fig. 8. Mohr–Coulomb failure envelopes for unreinforced clay–pumice mixtures

Table 4. Peak shear-strength parameters of unreinforced clay–pumice mixtures

Pumice content (%)	Peak shear strength, τ (kPa)			Cohesion, c (kPa)	Friction angle, φ (°)	R^2
	σ = 25 kPa	σ = 50 kPa	σ = 75 kPa			
0%	26.40	35.50	41.02	19.69	16.30	0.9804
10%	25.50	35.00	42.75	17.17	19.00	0.9966
20%	25.25	38.25	44.25	16.92	20.81	0.9567
30%	24.75	34.90	44.40	15.03	21.46	0.9996
40%	24.50	36.25	48.50	12.42	25.64	0.9999
50%	25.75	40.00	55.75	10.50	31.00	0.9992

The angular shape and rough vesicular surfaces of pumice made it less prone to particle sliding and rotation, promoted confinement-dependent mechanical interlocking, and encouraged the formation of a more continuous granular force transfer skeleton. These factors increased the mobilized frictional resistance and produced a relatively stable response after peak [24,25]. The Mohr-Coulomb failure envelopes in Fig. 8 and the parameters in Table 4 show strong linear relationships between normal stress and peak shear stress, with R^2 values ranging from 0.9567 to 0.9999. Further increasing the pumice content from 0% to 50% increased the friction angle from 16.3° to 31.0° (by approximately 90.2%), and the cohesion decreased from 19.69 to 10.50 kPa (by approximately 46.7%). The reduction in cohesion is due to the failure of the continuous clay-to-clay bonding network as the pumice particles gradually replace the fine-grained matrix. The angularity of the surface and porous nature of the pumice, on the other hand, made contact rough, against sliding and rotation, and confinement-dependent. The combination of these mechanisms is the reason for the steeper failure envelope and the transition from cohesion-dominated to friction-controlled behavior at high pumice contents.

3.3.2 Group 2 (Reinforced Samples)

The Mohr-Coulomb failure envelopes shown in Fig. 8 and the parameters in Table 4 have a strong linear relationship with the normal stress to the peak shear stress, R^2 from 0.9567 to 0.9999. Increasing the pumice content from 0% to 50% allowed us to increase the friction angle from 16.3° to 31.0°, by a factor of 90.2%, while the cohesion fell from 19.69 kPa to 10.50 kPa, by a factor of 46.7%.

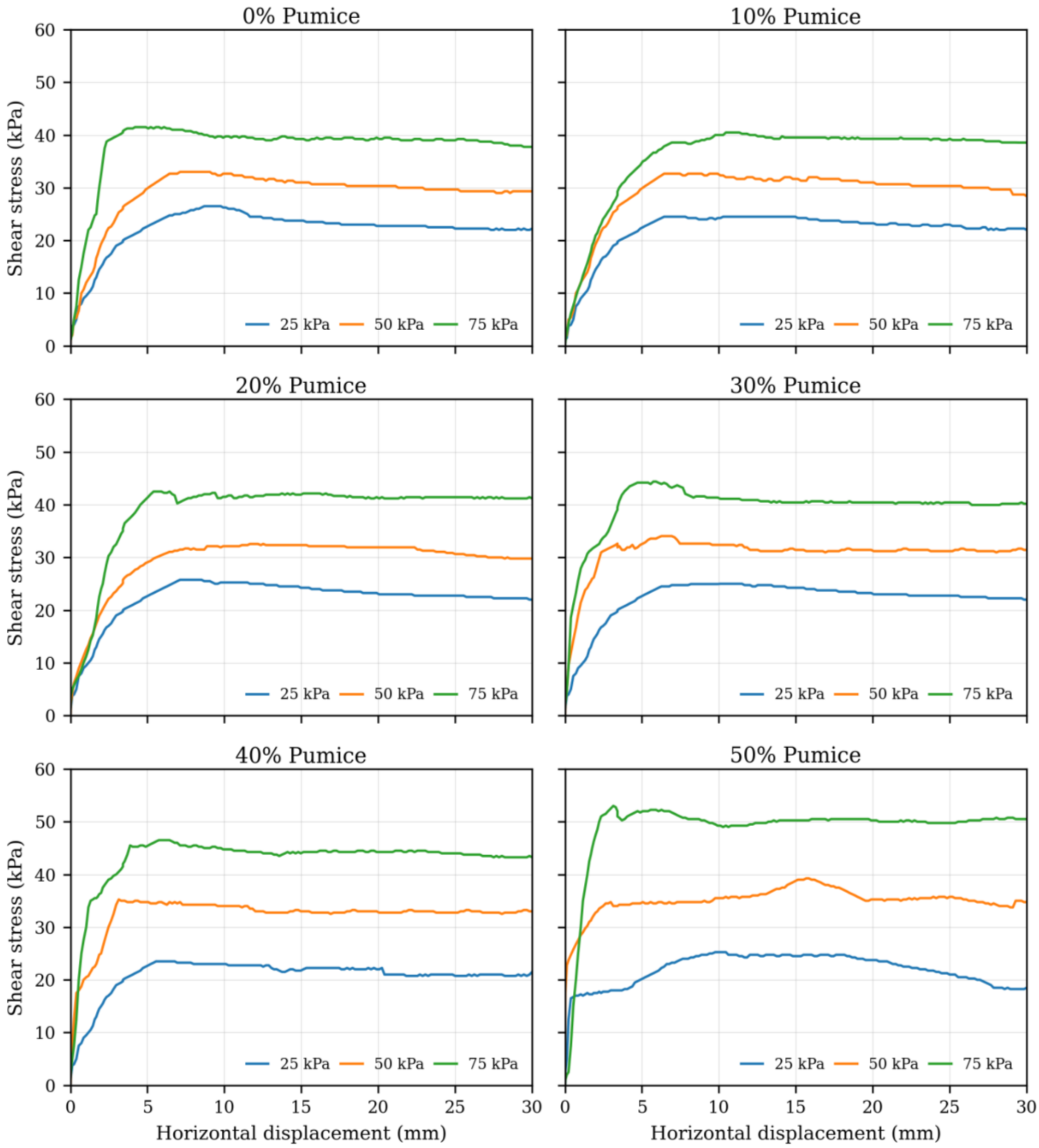

Fig. 9. Shear stress–horizontal displacement curves for reinforced clay–pumice mixtures

The reduction in apparent cohesion is because the continuous clay-clay bonding network was disrupted by the non-cohesive pumice particles as the fine-grained matrix became more and more pumice. On the other hand, the angularity of the surface asperities and porous nature of pumice caused the contact of particles to be rough and the friction to get shifted and rotated towards each other to be less and less, and therefore the interlocking between particles to be less and less. These are the mechanisms that lead to the steeper failure envelope and the transition from cohesion-dominated to friction-controlled behavior at high pumice contents. The failure-envelope regressions in Fig. 10 and the parameters in Table 5 show coefficients of determination ranging from R^2 = 0.9956 to 0.9998, indicating that normal stress is linear in the magnitude of interface shear. In Tables 4 and 5, the same stress levels, column sequence, units, and numerical precision are used to compare unreinforced and reinforced responses. The slope of the regression increased from 0.296 for natural clay to 0.555 for the 50% pumice mixture, corresponding to an interface friction angle that increased from 16.5° to 29.03°. This indicates that the thicker pumice content helped in the conversion of normal confinement to interface shear resistance through the roughness of the surface and particle interlocking. Reinforcement did not yield a uniform change in the fitted intercept. The apparent adhesion decreased from 19.69 to 19.38 kPa for the natural clay mixture and from 17.17 to 16.56 kPa for the 10% mixture, while small increases compared to the unreinforced values were found in 20-50% pumice. Their small increases are interpreted as localized locking of rough pumice particles against the polyethylene sheath, redistribution of clay near the strip, and regression variability corresponding to only three normal stress levels and not a systematic increase in cohesive bonding.

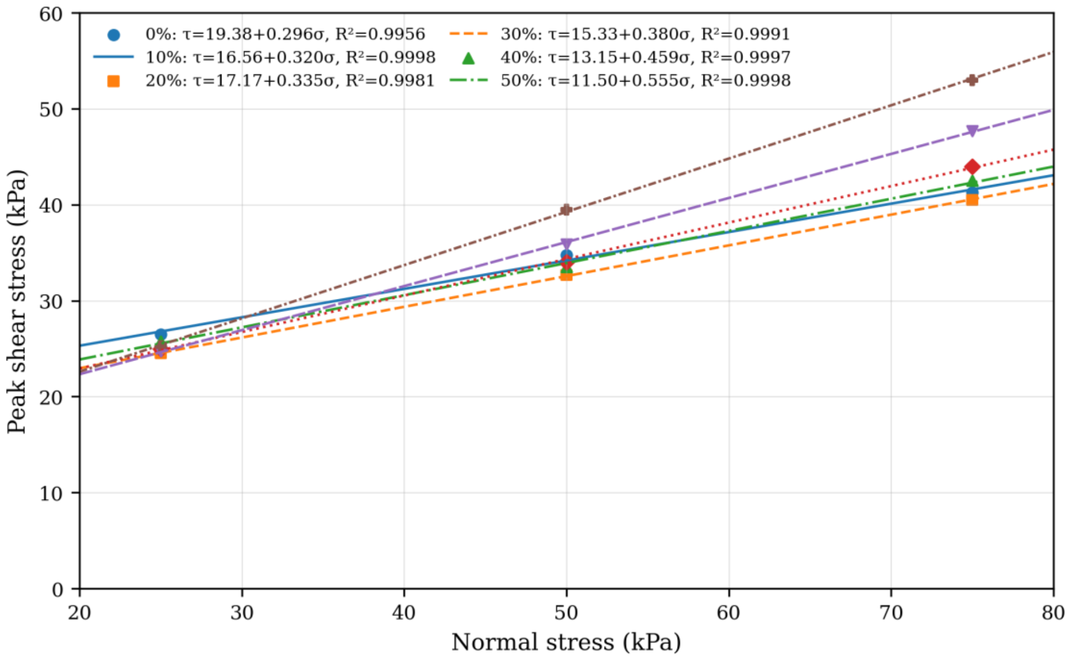

Fig. 10. Mohr–Coulomb failure envelopes for reinforced clay–pumice mixtures

Table 5. Peak interface shear-strength parameters of reinforced clay–pumice mixtures.

Pumice content (%)	Peak shear strength, τ (kPa)			Cohesion, c (kPa)	Friction angle, φ (°)	R^2
	σ = 25 kPa	σ = 50 kPa	σ = 75 kPa			
0%	26.50	34.75	41.30	19.38	16.50	0.9956
10%	24.50	32.67	40.50	16.56	17.75	0.9998
20%	25.75	33.50	42.50	17.17	18.52	0.9981
30%	25.00	34.00	44.00	15.33	20.80	0.9991
40%	24.75	35.86	47.70	13.15	24.66	0.9997
50%	25.25	39.50	53.00	11.50	29.03	0.9998

3.3.3 Interface Shear Strength Coefficient

The interface interaction coefficient, η, was used to compare the peak interface shear strength of the reinforced specimen with the peak shear strength of the corresponding unreinforced mixture at the same normal stress [16]. It was calculated using Eq. 4, where τ reinforced is the peak shear stress measured along the soil–geostrip interface and τ unreinforced is the peak shear stress of the unreinforced mixture:

$$\eta = \frac{\tau\, reinforced}{\tau\, unreinforced} \tag{4}$$

where η is the interaction coefficient at a specified normal stress, τ reinforced is the peak interface shear strength of the reinforced specimen, and τ unreinforced is the peak shear strength of the corresponding unreinforced specimen.

Fig. 11 and Table 6 show that the average η values ranged from 0.94 to 0.99, indicating that the soil–Geostrip interface generally mobilized a shear resistance close to the internal strength of the unreinforced mixtures. Similar interface responses have been reported to depend on confinement level and contact conditions for soil–geosynthetic direct shear testing [16]. Moreover, the very stable mean coefficients at 30-50% pumice suggest that the increase in granular content did not lead to a systematic deterioration of stress transfer. However, experimental uncertainty arises from specimen preparation, local density variation, pumice distribution, reinforcement alignment, and peak stress identification, for example. Therefore, we consider the 0.87 value as a single figure that requires replicate testing and not the material trend.

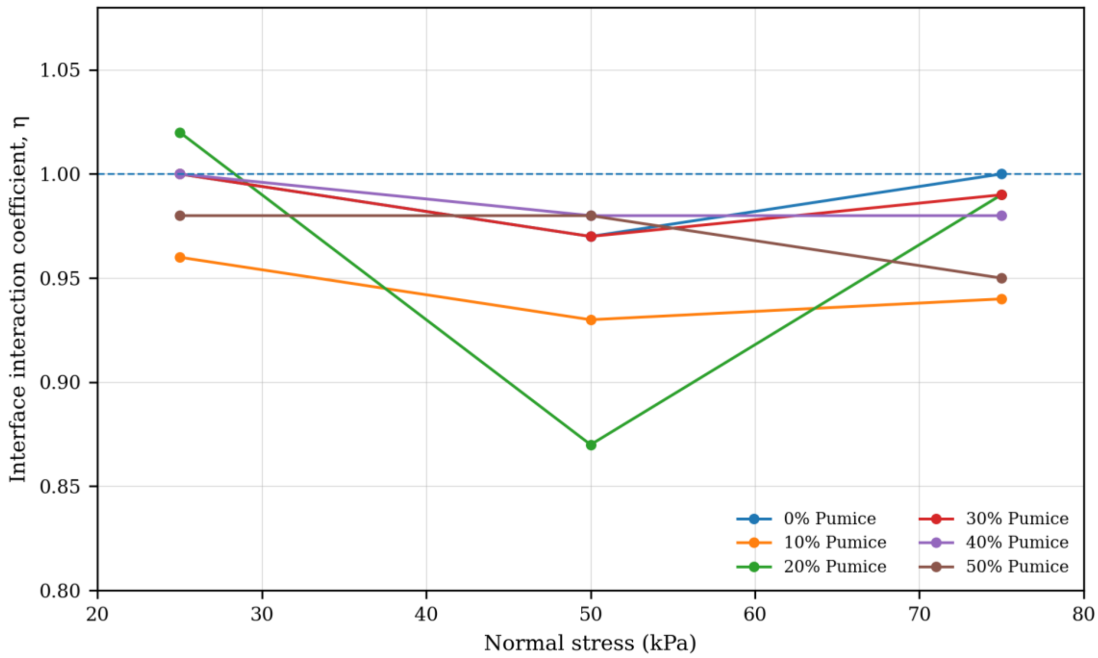

Fig. 11. Interface interaction coefficient versus normal stress for reinforced clay–pumice mixtures

The interface coefficient η reached 1.02 for the 20% pumice mixture under the lowest normal stress (25 kPa). Although interface coefficients are expected to be equal to or slightly less than unity, this increase may be due to localized mechanical interlocking between the pumice particles and the rough Geostrip surface under low confinement that can slightly increase the mobilized interface shear resistance. Since the increase above unity is only approximately 2%, it is also within the range of normal experimental variability. A localized decrease in the interface coefficient η was observed for the 20% pumice mixture at 50 kPa. It seems to be a case of transition of the mixture (the cohesive clay matrix but not the frictional Ponza skeleton is fully dominant). In intermediate confinement, the initial contact between the particles at low stress may be partially broken before enough normal stress is available to fully mobilize interface friction, leading to the interface efficiency being temporarily lower. As the normal stress is increased to 75 kPa, frictional contact increases and interparticle interlocking is improved, and the interface coefficient is recovered. Since this behavior was only observed for the 20% Ponza mixture, it should be understood as a local response of the transitional soil fabric rather than a general trend.

Table 6. Peak interface interaction coefficients at different normal stresses.

Pumice content (%)	η at 25 kPa	η at 50 kPa	η at 75 kPa	Average η
0%	1.00	0.97	1.00	0.99
10%	0.96	0.93	0.94	0.94
20%	1.02[a]	0.87[b]	0.99	0.96
30%	1.00	0.97	0.99	0.98
40%	1.00	0.98	0.98	0.98
50%	0.98	0.98	0.95	0.97

Notes: [a] Slightly above unity; possible local locking or experimental scatter. [b] Isolated low value; replicate testing is required to assess specimen variability.

4. Conclusions

In this study, we have studied the combined effects of pumice replacement and ParaWeb 2D reinforcement on compaction characteristics, soaked CBR, shear strength and soil–Geostrip interface behavior of Al-Amiriya clay through modified Proctor compaction and large-scale direct shear testing. Based on these experimental findings, we can draw the following conclusions:

- The addition of pumice gradually reduced the maximum dry unit weight but raised the internal friction angle. The maximum dry density decreased by about 10.9% when a pumice replacement is 50% and the friction angle increased from 16.3° to 31.0°. The combined effect decreased the active earth pressure, which indicates that pumice-modified clay has great potential as a lightweight reinforced backfill for MSE walls.
- The large-scale direct shear testing demonstrated a gradual transition from cohesion-controlled behavior to friction-controlled behavior as the pumice content increased. This transition reduced post-peak softening and produced a more stable shear response under higher normal stresses.
- The results of the experiments suggest that the most appropriate pumice content is based on the performance-based value rather than on the optimal replacement ratio. Although the 50% pumice mixture retained the highest friction angle and soaked CBR values, the 30% mixture retained the natural-soil cohesion of 76.3% and increased the friction angle by about 31.7% and the soaked CBR by about 138.4%. Therefore, it is good if the 30% mixture is the right balance of cohesion retention and frictional resistance, but the higher the pumice content, the more appropriate it is for a design in which maximum bearing capacity and weight reduction are the focus.
- The reinforced specimens had interface interaction coefficients of 0.94-0.99, indicating excellent compatibility with ParaWeb 2D and clay modified by pumice. The interface transferred shear stresses effectively with no significant loss of resistance, which indicates the suitability of the proposed system for reinforced soil applications.
- The proposed pumice–Geostrip system is a technically promising solution for lightweight embankments and MSE wall backfills constructed on Al-Amiriya clay or similar soils by reducing self-weight, enhancing soaked bearing capacity and efficient soil–reinforcement interaction. However, the economic feasibility should be examined according to the local material availability, transportation distance and project-specific costs.

The conclusions are limited to the tested soil type, pumice gradation, replacement ratios, normal-stress range, specimen preparation method, and loading conditions adopted in this study. Because pore-water pressures were not monitored and the selected shear rate was not established from specimen-specific consolidation characteristics, the measured shear parameters should be regarded as rate-dependent large-scale shear parameters rather than fully drained or undrained properties. Future research should investigate particle crushing, pullout resistance, long-term settlement, reinforcement creep, cyclic traffic and seismic loading, wetting–drying durability, freeze–thaw resistance where applicable, pore-water-pressure response, repeatability and uncertainty, and full-scale field performance.

Acknowledgement

This research was conducted as part of the requirements for a Master's degree in Civil Engineering. The authors thank the staff of Mustansiriyah University laboratories and Burj Babel Company for Studies and Scientific Research for facilitating the experimental work. Madhat Shakir Al-Soud and Qais S. Banyhussan contributed to the methodology and manuscript review; Sami S. Jasim conducted the experiments, analyzed the data, and prepared the original draft.

References

[1] Shimobe S, Spagnoli G. Some generic trends on the basic engineering properties of fine-grained soils. Environmental Earth Sciences. 2019;78:281. https://doi.org/10.1007/s12665-019-8266-4
[2] Zolfaghari Z, Mosaddeghi MR, Ayoubi S, Kelishadi H. Soil Atterberg limits and consistency indices as influenced by land use and slope position in western Iran. Journal of Mountain Science. 2015;12(6):1471-1483. https://doi.org/10.1007/s11629-014-3339-z
[3] Önalp A, Bol E, Özocak A, Sert S, Ural N, Arel E. Influence of index properties on the cyclic failure of fine-grained soils. Engineering Geology. 2023;317:107056. https://doi.org/10.1016/j.enggeo.2023.107056
[4] Lambe TW. The structure of compacted clays. Journal of the Soil Mechanics and Foundations Division. 1958;84(2):1654-1-1654-34. https://doi.org/10.1061/JSFEAQ.0000114
[5] Sherwood PT. Soil Stabilization with Cement and Lime: State-of-the-Art Review. Crowthorne: Transport Research Laboratory; 1993.
[6] Al-Waily MJ. Principles of Foundation Engineering. 4th ed. 2024. (In Arabic).
[7] Choo H, Hwang J, Choi Y, Lee C, Lee W. Geotechnical characteristics of volcanic beach sands with varying iron contents. Marine Georesources & Geotechnology. 2016;34(6):571-580. https://doi.org/10.1080/1064119X.2015.1043476
[8] Sayyah MA, Abrishami S, Dastpak P, Dias D. Behavior of volcanic ash-soil mixtures under one-dimensional compression testing. Scientific Reports. 2022;12:14524. https://doi.org/10.1038/s41598-022-18767-8
[9] Beyranvand A, Ghazavi M, Lajevardi SH, Mirhosseini SM. Laboratory large-scale pullout tests for evaluation of waste plastic bottles as transverse members on geogrid reinforcement. International Journal of Geosynthetics and Ground Engineering. 2022;8:43. https://doi.org/10.1007/s40891-022-00380-4
[10] Zhang WH, Wang BT, Zhang FH, Li SD. Test study on interaction characteristics between two-way geogrids and clay. Rock and Soil Mechanics. 2007;28(5):1031-1034.
[11] Coduto DP, Yeung MCR, Kitch WA. Geotechnical Engineering: Principles and Practices. Upper Saddle River: Prentice Hall; 1999.
[12] Budhu M. Soil Mechanics and Foundations. 3rd ed. Hoboken: John Wiley & Sons; 2011.
[13] Das BM. Advanced Soil Mechanics. 4th ed. Boca Raton: CRC Press; 2014.
[14] Das BM, Sobhan K. Principles of Geotechnical Engineering. 8th SI ed. Boston: Cengage Learning; 2014.
[15] Shukla SK, Yin JH. Fundamentals of Geosynthetic Engineering. London: Taylor & Francis; 2006.
[16] Liu CN, Zornberg JG, Chen TC, Ho YH, Lin BH. Behavior of geogrid-sand interface in direct shear mode. Journal of Geotechnical and Geoenvironmental Engineering. 2009;135(12):1863-1871. https://doi.org/10.1061/(ASCE)GT.1943-5606.0000150
[17] Koerner RM. Designing with Geosynthetics. 6th ed. Bloomington: Xlibris; 2012.
[18] Palmeira EM, Milligan GWE. Large-scale direct shear tests on reinforced soil. Soils and Foundations. 1989;29(1):18-30. https://doi.org/10.3208/sandf1972.29.18
[19] Zekkos D, Athanasopoulos GA, Bray JD, Grizi A, Theodoratos A. Large-scale direct shear testing of municipal solid waste. Waste Management. 2010;30(8-9):1544-1555. https://doi.org/10.1016/j.wasman.2010.01.024
[20] Choudhary AK, Krishna AM. Experimental investigation of interface behaviour of different granular soils and geosynthetics. International Journal of Geosynthetics and Ground Engineering. 2016;2:4. https://doi.org/10.1007/s40891-016-0044-8
[21] Banyhussan QS, Mosa MM, Hussein AN, Sigar EJ. Evaluating the shear strength of subbase-subgrade interface using a large-scale direct shear test. International Journal of Innovation in Engineering. 2023;3(1):35-47. https://doi.org/10.59615/ijie.3.1.35

[22] Sreelekshmypillai G, Vinod P. Prediction of CBR value of fine-grained soils at any rational compactive effort. International Journal of Geotechnical Engineering. 2019;13(6):560-565. https://doi.org/10.1080/19386362.2017.1374495
[23] Nagaraj HB, Suresh MR. Influence of clay mineralogy on the relationship of CBR of fine-grained soils with their index and engineering properties. Transportation Geotechnics. 2018;15:29-38. https://doi.org/10.1016/j.trgeo.2018.02.004
[24] Yin K, Fauchille AL, Di Filippo E, Kotronis P, Sciarra G. A review of sand-clay mixture and soil-structure interface direct shear tests. Geotechnics. 2021;1(2):260-306. https://doi.org/10.3390/geotechnics1020014
[25] Siahkouhi M, Pletzer C, Marcher T, Schneider-Muntau B. Investigation of shear-strength parameters of soil and soft-rock materials in the low-stress range. Geosciences. 2021;11(4):169.
[26] Aljboori W, Al-Soud M, Ali AM. Geotechnical properties of soil-lightweight aggregate mixtures. Engineering, Technology & Applied Science Research. 2025;15(1):20401-20408. https://doi.org/10.48084/etasr.9419
[27] Maccaferri. ParaWeb 2 Technical Data Sheet: Polymeric Geostrips for Reinforced Soil Applications. Revision 08; 2015. Available at: https://gpil.co.nz/wp-content/uploads/2022/03/TDS-PARAWEB-2_rev08-20151016.pdf.
[28] Deiminiat A, Li L, Zeng F. Experimental study on the minimum required specimen-width-to-maximum-particle-size ratio in direct shear tests. CivilEng. 2022;3(1):66-84. https://doi.org/10.3390/civileng3010005
[29] Saltan M, Kavlak Y, Ertem FS. Utilization of pumice waste for clayey subgrade of pavements. Journal of Materials in Civil Engineering. 2011;23(12):1616-1623. https://doi.org/10.1061/(ASCE)MT.1943-5533.0000336
[30] Nasiri H, Khayat N, Nazarpour A. Assessing one-year effects of 10% pumice powder on strength and microstructure of contaminated clay (case study: Ahvaz Project, Iran). Case Studies in Construction Materials. 2024;21:e03892. https://doi.org/10.1016/j.cscm.2024.e03892
[31] Chai J-C, Saito A. Interface shear strengths between geosynthetics and clayey soils. International Journal of Geosynthetics and Ground Engineering. 2016;2:19. https://doi.org/10.1007/s40891-016-0060-8
[32] Muluti SS, Kalumba D, Sobhee-Beetul L, Chebet F. Shear strength of single- and multi-layer soil-geosynthetic and geosynthetic-geosynthetic interfaces using large direct shear testing. International Journal of Geosynthetics and Ground Engineering. 2023;9:33. https://doi.org/10.1007/s40891-023-00450-1